

Degradation Behavior of GO-ternary Blended Nano-concrete Composites under Accelerated Sulfuric Acid Attack

Abdullah Anwar¹, Xuemei Liu¹ and Lihai Zhang¹

¹Department of Infrastructure Engineering, The University of Melbourne, Parkville 3010, Australia
abdullah.anwar@student.unimelb.edu.au (A.Anwar), lihzhang@unimelb.edu.au (L.Zhang),
xuemei.liu@unimelb.edu.au (X.Liu) (Corresponding author)

Abstract. *Biogenic corrosion of concrete in wastewater sewer systems is caused by the in-situ production of sulfuric acid (H₂SO₄) formed by the bacterial action is considered the principal cause of structural degradation. The intense corrosive environment disintegrates the service lifespan of concrete structures significantly sooner in its advanced state, resulting in structural collapse within 10-20 years and jeopardising its durability. Thus, the degradation of concrete structures in the aggressive acidic environment of sewerage systems remains a global concern for industries and stakeholders, resulting in economic losses of several billion dollars annually. This research experimentally investigates the degradation behavior of developed ternary blended nano-concrete composites reinforced with graphene oxide (GO-TBNCCs) under accelerated H₂SO₄ exposure (pH 1.0) for 28 days and 90 days. The experimental results revealed that TBNCCs reinforced with GO are more resistant to aggressive acidic attack in contrast to its control composites, hence increasing its acidic resistivity performance with lower degradation depth that may cater to the durability problem of concrete structures in the wastewater sewer systems.*

Keywords: *Degradation Depth; Durability, Sulfuric Acid; Sewerage System; Ternary Blended Concrete; Supplementary Cementitious Materials; Graphene Oxide.*

1 Introduction

Concrete is a multiphase, porous, strongly basic material (pH ~13.0) widely used in constructing sewage treatment plant facilities (Zhao 2020). However, the very harsh environment surely jeopardizes the durability of concrete (Teplý et al. 2018). Biogenic sulfuric acid (BSA) attack is one of the leading causes of concrete failure in sewerage system (Parker 1945, Mori et al. 1991). In a BSA attack, the principal corrosive element is hydrogen sulfide (H₂S), which transforms into sulfuric acid (H₂SO₄) by microorganisms and causes rapid degradation of concrete structures with reduced pH of 1.0 or even lower (Taheri 2021). The decreased alkalinity of concrete directly impacts its degradation behavior in sewage environments (Liu et al. 2022). As a consequence, concrete structures have a shorter lifespan and incur extraordinarily high financial costs (in the millions of dollars) for their annual repair and maintenance across the globe (Gu et al. 2019). The deterioration of cementitious composites as a result of BSA attack is described in our previous research work (Anwar et al. 2022). Additionally, a minimum service life of 50 years is required for concrete structures in wastewater systems, as required by standards for design and maintenance (Woyciechowski et al. 2019, EN 1504-10:2017). The extreme hazardous atmosphere in the sewerage system, however, causes concrete infrastructures to disintegrate much sooner, causing them to fail structurally within 10–20 years and jeopardizing their durability (Davies et al. 2001). Therefore,

in light of the increasing demand for structures with longer service life and lower maintenance requirements, the durability of concrete material is becoming increasingly important.

An important performance parameter of structural materials is their acid resistance when applied to sewerage systems with aggressive environments (Lee and Lee 2016). A more promising approach for enhancing concrete durability when exposed to low pH environments is by optimizing the concrete mix with supplementary cementitious materials (SCMs) (Monteny et al. 2003). As such, Wang et al. (Wang et al. 2020) discussed the different mitigation approach toward concrete biogenic corrosion and identified that the usage of SCMs illustrates better performance (especially at low pH 1-4), more convenience and easy to apply for improving the durability purpose. Jiang et al. (Jiang et al. 2014) suggested the use of low iron content cementitious component that may reduce the iron-induced micro cracking and probably increase the concrete resistance to sulfide corrosion in sewerage system. Additionally, Woyciechowski et al. (Woyciechowski et al. 2021) recommended further studies considering concrete mix design of minimum strength class C35/45 with lower w/c ratio (≤ 0.4) and pozzolanic mixtures (preferably GGBFS) for wastewater sewer structures. As higher w/c ratio will make the concrete matrix more porous resulting in rapid transport of hazardous chemicals and increasing the rate of concrete degradation. In comparison with binary blended concrete systems, ternary blended concrete composites (blends of cement with fly ash (FA) and ground granulated blast furnace slag (GGBFS)) exhibited improved degradation resistance (Rivera and Miguel 2020). The ternary-blended system could make the use of the advantageous properties of the improved workability and low environmental impact of FA while maintaining adequate strength and durability properties with a higher level of cement replacements through the use of GGBFS (Radwan et al. 2022). However, at higher replacement proportion of FA and GGBFS results in reduced performance of ternary blended matrix (Muthu et al. 2021). Further, the use of GGBFS may reduce the iron-induced micro-cracking due to lower iron content (~1%) and probably increase the concrete resistance to acidic corrosion. Additionally, further investigation on the durability performance of ternary blended concrete composites (TBCCs) were also recommended (Gholampour and Ozbakkaloglu 2017). Alternatively, nano-scale treatment of concrete matrix present an opportunity to achieve a highly durable and long-lasting construction material that can significantly strengthen the overall performance of concrete composites (Mousavi et al. 2020).

Graphene Oxide (GO) is one such promising nanomaterial that has attracted lots of attention due to its better performance in improving the characteristics of concrete composites (Idukuri and Nerella 2021, Anwar et al. 2023) Fig.1 illustrates the GO hexagonal structure composed of carbon atoms covalently linked to oxygen atoms such as hydroxyls (-OH), epoxides (-O-), carboxyls (-COOH), and ketone carbonyls (-COO) (Anwar et al. 2023, Chuah et al. 2014, Anwar et al. 2020). GO features a larger surface area (~1700 m²/g), an increased aspect ratio (~45000), greater tensile strength (~130 MPa), smaller thickness (0.7-1.0nm), and a higher Young's modulus (210-470 GPa) (Muthu et al. 2021). The enhanced surface availability adorned with oxygen-derived functional groups is primarily responsible for its novel functionality and improved concrete composite performance (Pettitt and Lead 2013). However, limited studies have been conducted concerning the degradation resistance of blended concrete composites tailored with GO nanomaterials in aggressive acidic environments (Idukuri and Nerella 2021, Anwar et al. 2023, Muthu et al. 2021). As a way to fill this research gap, this

study experimentally investigated the degradation behavior of developed graphene oxide ternary blended nano-concrete composites (GO-TBNCCs) exposed to accelerated sulfuric acid (H_2SO_4) attack (pH 1.0) over a period of 28 days and 90 days

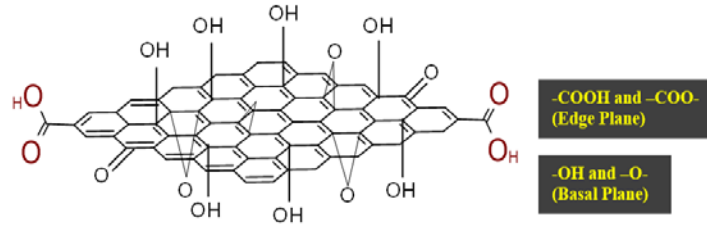


Figure 1. Graphical illustration of GO-molecular structure (Anwar et al. 2023, Li et al. 2013)

2 Materials and Methods

2.1 Material and Mix Proportions

A General Purpose (GP) type grade OPC in compliance with AS 3972 (AS 3972-2010:2010) was used. The SCMs includes GGBFS according to AS 3582.2 (AS 3582.2 – 2001:2001) and FA (Class F) conforming to AS 3582.1 (AS 3582.1-1998:1998) were used. The chemical composition of these raw materials are shown in Table 1. The water absorption for coarse and fine aggregate was observed as 1.13% and 1.58%. The chemical admixture includes polycarboxylate ether based superplasticizer (PCE-SPs) with a solid content of 36-38 wt%, conforming to AS1478 (AS 1478.1:2000). The physical parameters and elemental properties of GO are listed in Table 2. The powdered form of GO-nanomaterial in powder form was supplied by Ad-Nano Technologies Pvt. Ltd. (India) with a purity of ~99%. The physical parameters and elemental properties of GO are listed in Table 2. Fig. 2 shows the visual appearance and SEM-imaging of GO-nanosheets. An analytical reagent grade H_2SO_4 (98% concentration) and Phenolphthalein (Ph.) solution (pH 8.2-9.8) was provided by local supplier.

Table 1: Chemical compositions of GGBFS, FA, and OPC (ED-XRF spectrometer, MCFP, UniMelb)

Binder	Composition (wt% as oxide)										
	SiO ₂	Al ₂ O ₃	CaO	MgO	Fe ₂ O ₃	SO ₃	MnO	SrO	K ₂ O	TiO ₂	ZnO
GGBFS	31.57	10.90	43.98	5.58	0.37	5.67	0.40	0.10	0.45	0.66	-
FA	54.33	26.28	6.71	1.24	8.12	0.29	0.13	0.05	0.84	1.84	0.02
OPC	16.99	3.63	69.61	1.18	3.50	3.83	0.07	0.09	0.37	0.22	0.07

Table 2: Physical and Chemical properties of GO nanosheets (Ad-Nano Technologies, India)

Appearance	Physical Parameters					Elemental Composition (%)				
	Purity	Thickness	Flake Size	Number of Layers	Surface Area	Carbon	Oxygen	Hydrogen	Nitrogen	Sulfur
Black Powder	~99%	~0.8-2nm	~5-10 μ m	1-3	110-250 m ² /g	~60-80	~15-32	~1-2	~1-2	<1

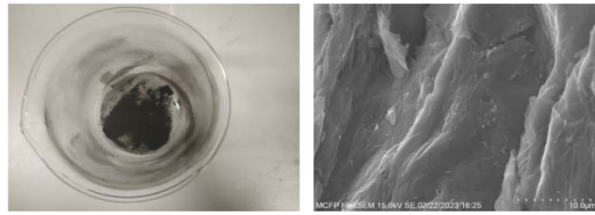


Figure 2. GO (a) Physical Appearance (black powder); (b) SEM imaging (SE-mode, MCFP, UniMelb)

The ternary blended mix was developed using the mix proportions listed in Table 3. The level of SCMs is in accordance with AS/NZS 4058:2007 (AS/NZS 4058:2007), BS-EN 206:2013 (BS-EN 206:2013), and in agreement with the literature (Radwan et al. 2022, Gholampour and Ozbakkaloglu 2017, Matějková et al. 2022) The replacement mass ratio of GGBFS to cement was ≤ 1.0 . Additionally, PCE-SPs is used as the surface modifier for GO to improve its dispersion in the concrete matrix. Prior mixing to concrete, GO-PCE-SPs colloidal suspension is processed through three stage treatment of magnetic stirrer (2hrs@1000rpm), ultrasonication (10min.@5sec. pulse) and high shear mixer (2000rpm@15min.) for its better dispersion in concrete mix. A complete set of six mixes were produced, comprising three reference and three GO-mixes at a constant water-cementitious (w/cm) ratio of 0.38. For each combination, 06 cylinders (75 mm diameter x 150 mm height) were formed and tested on cured concrete at 28 days and 90 days acid exposure.

Table 3: GO-TBNCCs – Mix Proportions

Mix ID	Factors (Variables)			Cement (kg/m ³)	FA (kg/m ³)	GGBFS (kg/m ³)	GO (gm/m ³)	CA (kg/m ³)	FA (kg/m ³)	Water (kg/m ³)
	FA (%)	GGBFS (%)	GO (%)							
20F20GB	20	20	0	292.2	97.4	97.4	0	887	927	185.06
20F30GB	20	30	0	243.5	97.4	146.1	0	887	927	185.06
20F40GB	20	40	0	194.8	97.4	194.8	0	887	927	185.06
20F20GB 275GO	20	20	0.0275	292.2	97.4	97.4	133.93	887	927	185.06
20F30GB 275GO	20	30	0.0275	243.5	97.4	146.1	133.93	887	927	185.06
20F40GB 275GO	20	40	0.0275	194.8	97.4	194.8	133.93	887	927	185.06

Note: FA – Fly ash; GGBFS – Ground granulated blast furnace slag; GO – Graphene Oxide;

2.2 Experimental Setup

After 28 days of water immersion, the top and bottom faces of the cylindrical samples were coated with non-reactive silicone gel before the sulfuric acid exposure, as shown in Fig.3b. The sealed surface will ensure the acidic penetration mostly from the radial direction instead of the vertical path. Following that, the specimens are submerged on curved surfaces in an accelerated H₂SO₄ bath solution (pH 1.0, 0.05mol/L) for the requisite 28 and 90 days of acidic conditions. The accelerated H₂SO₄ solution was prepared in a 128L HDPE container filled with ~60L diluted acidic solution. Using a portable pH/ORP meter (HI 2211 pH/ORP meter), the pH level of the acidic bath solution was checked three times per week, and the solution was physically agitated periodically to prevent the formation of strong ionic gradients. Moreover, to maintain the desired pH level of 1.0, ~35-40% concentrated H₂SO₄ (98%) was added periodically (1-2 times a week) to the bath solution.

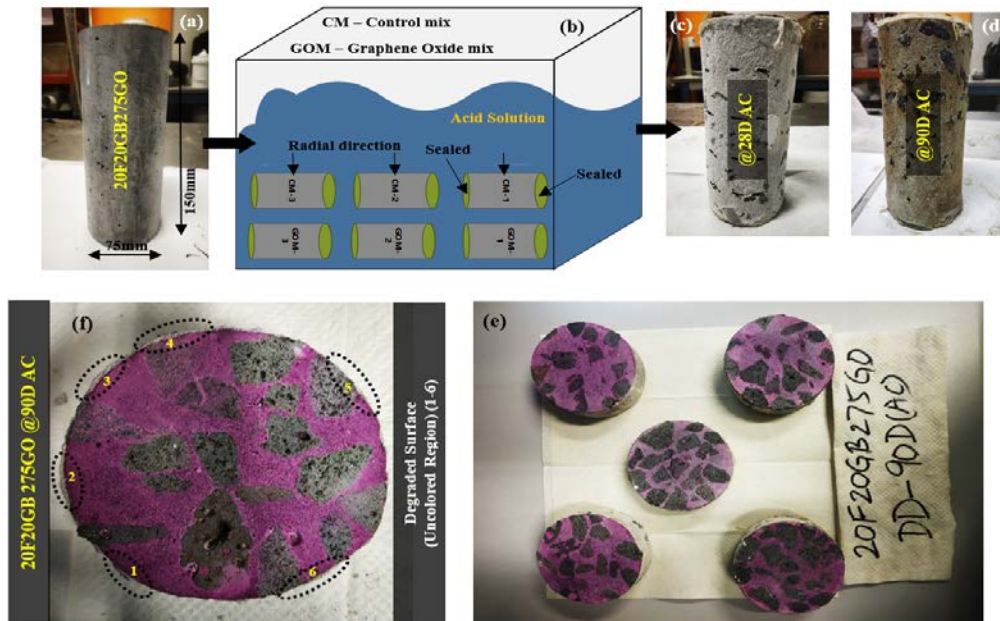


Figure 3. Degradation depth experimental process (a) cylindrical sample after 28d water curing; (b) graphical illustration of samples immersed on curved faces in the acid bath; (c), (d) degraded samples after 28d and 90d acid attack; (e) cylindrical discs obtained from splitting the sample by using diamond saw; (f) Ph. solution test to examine the extent of degraded surface (Francis lab, UniMelb)

2.3 Degradation Depth Measurement

Degradation depth refers to the zone in which material properties have altered, or surface alkalinity has changed (Ren et al. 2020, Koenig and Dehn 2016). In contrast to mass and strength changes, it is considered a more accurate indicator of degradation severity and kinetics (Ren et al. 2020). The degradation depth measurement is intended to provide more detailed information on how concrete composites respond to acid attacks by quantifying their acidic resistivity performance (ARP). Following BS EN 14630:2006 (BS EN 14630:2006) and as reported in the literature (Ren et al. 2022), degradation depth was measured on cylindrical specimens exposed to aggressive H_2SO_4 attack. Following acidic immersion, samples were removed from the bath solution and oven dried for 24 hours at $105 \pm 5^\circ C$. On the testing day, the core specimen was cut into the cylindrical disc (each of 30mm thickness) by using a diamond-saw and cleaned with water for degradation measurements, as shown in Fig.3e. A minimum of 15-20 measurement points per specimen disc are considered at equal intervals. As an indicator of degradation depth; each disc sample was treated with Phenolphthalein (Ph.) solution to examine the degraded and undegraded zones (Fig.3f). Change in pH via the use of Ph. reagent is a widely adopted method to distinguish between degraded and undegraded zone (Gu et al. 2019, Gu et al. 2020). The degraded and undegraded regions of the concrete surface may turn colorless and purple upon encountering with Ph. solution, respectively (Fig.4b). Thus, pH 8.3 is regarded as a turning point to distinguish between degraded and un-degraded area. Degradation depth was measured by using Carl Zeiss optical microscope (Wet Lab, UniMelb) (Fig.4a). Dissolved Depth (DD) is the specimen circumferential part that dissolves in acidic solution due to acidic attack and is calculated by measuring the difference between the original

and reduced diameter of the specimens. For apparent degradation depth (ADD), the borders of the transformed zone were determined, and the region of discoloration visible in the image was processed using an imaging application to precisely measure the ADD. Therefore, the total degradation depth (TDD) refers as the quantitative summation of DD and ADD as shown in Fig.4b. The final degradation depth is the average value of the TDD for all three cylinders from each mix group.

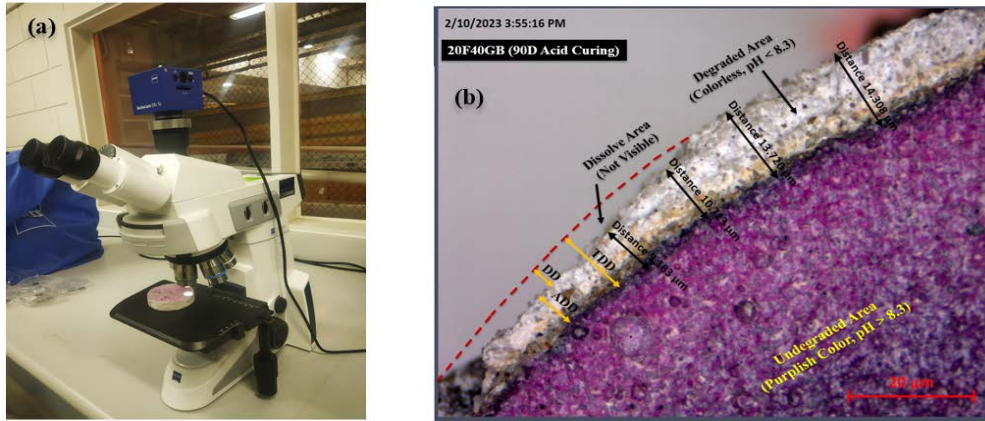


Figure 4. Degradation kinetics measurement (a) using an optical microscope; (b) microscopic view illustrating the degraded and undegraded area with DD, ADD, and TDD (Wet lab, UniMelb)

3 Results and Discussion

Fig. 5 depicts the Ph. test performed on the samples cut-surface for all concrete blends subjected to accelerated H_2SO_4 attack. As shown in Fig.5 and Fig.6a, GO-TBNCCs have a significantly lower degradation depth than ternary blended mixes. In the 28days acid attack, mix 20F40GB275GO recorded the lowest DD and ADD measurements of 0.48mm and 5.65 μ m, respectively. Similar results can be observed at 90 days, with minimum DD and ADD of 0.37mm and 4.82 μ m, respectively. Compared to the control mix 20F40GB, this degradation effect is about 72.75% lower at 28 days and 86.01% lower at 90 days of acid exposure. Therefore, the mix 20F40GB275GO demonstrated the most significant reduction in TDD of concrete composites compared to other mixes, as shown in Table 4.

Table 4: GO-TBNCCs – Reduction in TDD

Mix ID	20F40GB275GO (% reduction in contrast to)	
	28d AC	90d AC
20F20GB	81.96	90.16
20F30GB	79.75	87.98
20F40GB	72.75	86.01
20F20GB 275GO	68.74	76.45
20F30GB 275GO	28.49	21.97

As a result of the synergistic mechanism of the GO-GGBFS-FA system in a concrete matrix, the TDD of GO-concrete specimens is reduced after the acidic attack. The GGBFS-FA system contains higher alumina (Al) and silica (Si)-content and a lower proportion of calcium (Ca) (Table 1). The higher alumina content results in more intensive cross-linked alumina gel phases,

which are chemically more stable and resistant to acid attacks (Aboulela et al. 2021). Furthermore, concrete matrix with higher Si and lower Ca content has greater pH stability with increased resistance to decalcification and leaching (Ren et al. 2022). Moreover, the pozzolanic activity of FA and GGBFS coupled with GO-nanosheets heals the concrete matrix internally at nano-scale to micro-scale via multiple reinforcing mechanisms of filling, bonding, and nucleation processes (Anwar et al. 2023, Lv et al. 2013). Through the nano-filling effect, the 2-D wrinkled morphology of the GO surface stimulates the hydration reaction process of cement and facilitates the development of hydration products into the pores of cement composites. The nano-filling action forms a nanosheet covering over the cement grains, which act as a protective barrier, preventing the penetration of corrosive acidic ions, reducing the intensity of hazardous pores, and increasing the proportion of gel pores (1-10nm) (Habibnejad et al. 2020). This results in a substantially denser concrete matrix microstructure and avoids the dissipation of alumina gel phases generated by the GGBFS and FA blended system. Additionally, the surface pH test witnessed that including GO-nanosheets improves the alkalinity of concrete in the degraded zone with retained surface pH of more than 8.0 in contrast to control mixes (Fig. 6b), hence improving the degradation performance of GO-TBNCCs against aggressive acidic attack.

Zone 1	Zone 2
Un-degraded area (pH > 8.3)	Degraded Area (pH < 8.3)

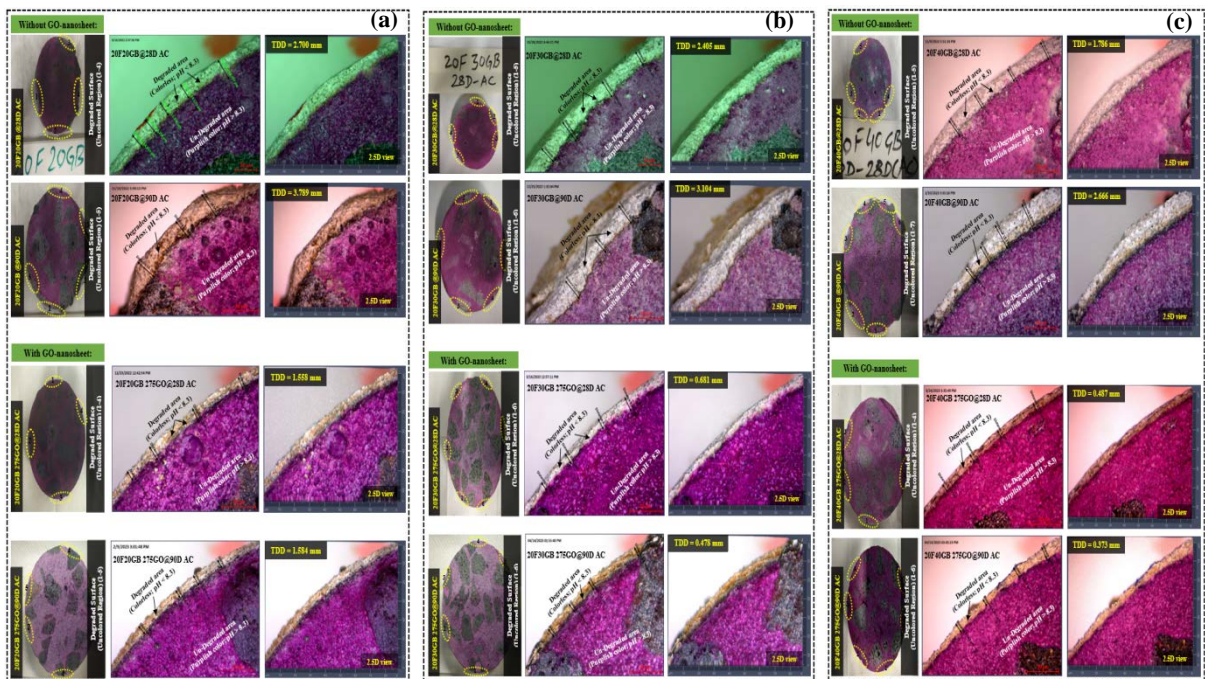


Figure 5. Degradation depth measurement of GO-TBNCCs samples via optical microscope @28d and 90d acid attack (a)20F20GB and 20F20GB275GO; (b)20F30GB and 20F30GB275GO; (c)20F40GB and 20F40GB275GO

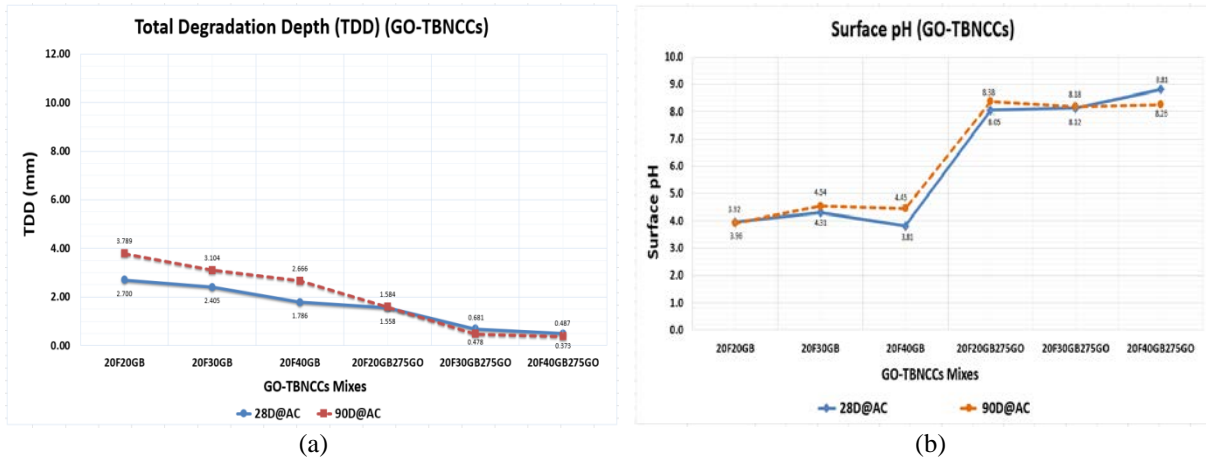


Figure 6. GO-TBNCCs mixes @28d and 90d acid attack (a) Degradation Depth; (b) Surface pH

4 Cost-benefit Analysis

Table 5 evaluates the cost study of various TBNCCs mixtures reinforced with GO-nanomaterial based on commercialized market rates of the materials. The economy index (corrosion depth/cost per m³ of concrete) for mix 20F40GB275GO with highest ARP is only 11.45% of the cost incurred for the control mix. This will improve the economic life of concrete structures used in sewerage systems.

Table 5: Cost analysis of GO-TBNCCs mixes (in per m³)

Materials (kg)	Cost (AUD/kg)	GO-TBNCCs Mixes					
		20F20GB	20F30GB	20F40GB	20F20GB 275GO	20F30GB 275GO	20F40GB 275GO
OPC	0.50	146.10	121.75	97.40	146.10	121.75	97.40
Fly ash	0.52	50.648	50.648	50.648	50.648	50.648	50.648
GGBFS	0.65	63.31	94.965	126.62	63.31	94.965	126.62
FA	0.49	454.23	454.23	454.23	454.23	454.23	454.23
CA	0.42	372.54	372.54	372.54	372.54	372.54	372.54
SPs	12.00	58.44	67.20	70.128	93.504	181.164	201.618
GO	1.06 per gm	0	0	0	141.961	141.961	141.961
Water	0.0029	0.536	0.536	0.536	0.536	0.536	0.536
Total (AUD)	-	1145.804	1161.869	1172.102	1322.828	1417.793	1445.552
Corrosion depth (mm@90d)	-	3.789	3.104	2.666	1.584	0.478	0.373
EI for CR	-	0.00331	0.00267	0.00227	0.00119	0.00034	0.00026

Note: FA-Fine aggregate; CA-Coarse aggregate; GO-Graphene oxide; SP-Superplasticizer; CR-Corrosion rate; EI-Economy index

5 Conclusions

The degrading behavior of GO-TBNCCs subjected to accelerated acidic attack for 28 days and 90 days immersion period was investigated and compared in this research. The following conclusion may be drawn from this study:

- GO-TBNCCs demonstrated greater ARP after 28 days and 90 days of exposure, as shown by degradation depth measurements (Fig.6a). Among all, the mix 20F40GB275GO was deemed to be the optimal proportion with the maximum reduction

in degradation depth. This may be computed based on the evaluated performance of ~73% (@28d) and ~86% (@90d) drop in degradation depth compared to the control mixes (Table 4).

- Overall, based on the degradation depth investigation, the ARP of GO-TBNCCs can be arranged as 20F40GB275GO (max.) > 20F30GB275GO > 20F20GB275GO > 20F40GB > 20F30GB > 20F20GB (min.) (Fig. 5 and 6).
- The synergistic effect of the GO-GGBS-FA three-phase system may develop a protective layer in the concrete matrix that reduces the depth of the degraded zone and increases the area of the un-degraded (sound) zone with densified microstructure, thereby enhancing the ARP of GO-TBNCCs (Fig. 5).
- Based on the experimental findings, GO-TBNCCs may be considered as a potentially materialistic and cost-effective solution to the durability problem of critical infrastructures exposed to corrosive environments, like sewerage systems and marine structures.

Acknowledgements

The authors would like to acknowledge the Department of Infrastructure Engineering of the University of Melbourne (UniMelb), Australia, for facilitating this research study. The test on concrete samples was performed in the Francis Laboratory at the University of Melbourne (UniMelb), Australia. The Materials Characterisation and Fabrication Platform (MCFP) at the University of Melbourne for microscopic GO-nanosheet analysis.

Funding

The authors would like to thank the University of Melbourne (UniMelb), Australia, for financing the research project under the Melbourne Research Scholarship (2022) and the Sir William Foster Stawell Scholarship (2023).

ORCID

Abdullah Anwar: <https://orcid.org/0000-0002-0369-3119>

Xuemei Liu: <https://orcid.org/0000-0001-6400-8608>

Lihai Zhang: <https://orcid.org/0000-0002-1282-992X>

References

- Zhao L, Guo X, Song L, Song Y, Dai G, Liu J. (2020). *An intensive review on the role of graphene oxide in cement-based materials*. Constr Build Mater, 241, 117939. doi:10.1016/j.conbuildmat.2019.117939
- Teply B, Rovnaniková M, Routil L, Schejbal R. (2018). *Time-Variant Performance of Concrete Sewer Pipes Undergoing Biogenic Sulfuric Acid Degradation*. J Pipeline Syst Eng Pract. 9(4), 04018013. doi:10.1061/(asce)ps.1949-1204.0000327
- Parker CD. (1945). *The Isolation of a Species of Bacterium associated with the Corrosion of Concrete exposed to Atmospheres containing Hydrogen Sulphide*. Concrete, 23(2), 81-90. doi:https://doi.org/10.1038/icb.1945.13
- Mori T, Nonaka T, Tazaki K, Koga M, Hikosaka Y, Noda S. (1991). *Interactions of nutrients, moisture and pH on microbial corrosion of concrete sewer pipes*. Water Res, 26(1), 29-37. doi:https://doi.org/10.1016/0043-1354(92)90107-F
- Taheri S, Giri P, Ams M, et al. (2021). *Migration and formation of an iron rich layer during acidic corrosion of concrete with no steel reinforcement*. Constr Build Mater, 309, 125105. doi:10.1016/j.conbuildmat.2021.125105
- Liu H, Wang Y, Ren X, Xu H, Chen J. (2022). *Study on the transformation of Zn, Mn and Cr during sewage sludge combustion*. Process Saf Environ Prot, 161, 819-826. doi:10.1016/j.psep.2022.03.081
- Gu L, Bennett T, Visintin P. (2019). *Sulphuric acid exposure of conventional concrete and alkali-activated concrete: Assessment of test methodologies*. Constr Build Mater, 197, 681-692. doi:10.1016/j.conbuildmat.2018.11.166
- Anwar A, Liu X, Zhang L. (2022). *Biogenic corrosion of cementitious composite in wastewater sewerage system – A review*. Process Saf Environ Prot, 165, 545-585. doi:10.1016/j.psep.2022.07.030
- Woyciechowski P, Adamczewski G, Łukowski P. (2019). *Chemical corrosion of concrete tank in sewage treatment*

- plant as the cause of failure. MATEC Web Conf - ICSF 2019, 284, 07007. doi:10.1051/mateconf/201928407007
- EN 1504-10 (2017). *Products and Systems for the Protection and Repair of Concrete Structures - Definitions, Requirements, Quality Control and Evaluation of Conformity - Part 10: Site Application of Products and Systems and Quality Control of the Works*.
- Davies JP, Clarke BA, Whiter JT, (2001). Cunningham RJ. *Factors influencing the structural deterioration and collapse of rigid sewer pipes*. Urban Water, 3(1-2), 73-89. doi:10.1016/S1462-0758(01)00017-6
- Lee NK, Lee HK. (2016). *Influence of the slag content on the chloride and sulfuric acid resistances of alkali-activated fly ash/slag paste*. Cem Concr Compos, 72:168-179. doi:10.1016/j.cemconcomp.2016.06.004
- Monteny J, De Belie N, Taerwe L. (2003). *Resistance of different types of concrete mixtures to sulfuric acid*. Mater Struct Constr, 36(258), 242-249. doi:10.1617/13766
- Wang T, Wu K, Kan L, Wu M. (2020). *Current understanding on microbiologically induced corrosion of concrete in sewer structures: a review of the evaluation methods and mitigation measures*. Constr Build Mater, 247, 118539. doi:10.1016/j.conbuildmat.2020.118539
- Jiang G, Wightman E, Donose BC, Yuan Z, Bond PL, Keller J. (2014). *The role of iron in sulfide induced corrosion of sewer concrete*. Water Res, 49, 166-174. doi:10.1016/j.watres.2013.11.007
- Woyciechowski P, Łukowski P, Szmigiera E, Adamczewski G, Chilmon K, Spodzieja S. (2021). *Concrete corrosion in a wastewater treatment plant – A comprehensive case study*. Constr Build Mater, 303, 124388. doi:10.1016/j.conbuildmat.2021.124388
- Rivera RA, Miguel Á. (2020). *Granulated Blast-Furnace Slag and Coal Fly Ash Ternary Portland Cements Optimization*. Sustainability, 12(4), 1-15. doi:10.3390/su12145783
- Radwan MKH, Onn CC, Mo KH, Yap SP, Chin RJ, Lai SH. (2022). *Sustainable Ternary Cement Blends with High-Volume Ground Granulated Blast Furnace Slag–Fly Ash*. Vol 24. doi:10.1007/s10668-021-01633-4
- Muthu M, Yang EH, Unluer C. (2021). *Effect of graphene oxide on the deterioration of cement pastes exposed to citric and sulfuric acids*. Cem Concr Compos, 124, 1-13. doi:https://doi.org/10.1016/j.cemconcomp.2021.104252
- Gholampour A, Ozbakkaloglu T. (2017). *Performance of sustainable concretes containing very high volume Class-F fly ash and ground granulated blast furnace slag*. J Clean Prod, 162, 1407-1417. doi:10.1016/j.jclepro.2017.06.087
- Mousavi SS, Mousavi Ajarostaghi SS, Bhojaraju C. (2020). *A critical review of the effect of concrete composition on rebar–concrete interface (RCI) bond strength: A case study of nanoparticles*. SN Appl Sci, 2(5), 1-23. doi:10.1007/s42452-020-2681-8
- Idukuri CSR, Nerella R. (2021). *Enhanced Transportation Properties of Graphene Oxide based Cement Composite Material*. J Build Eng, 37, 1012174. doi:10.1016/j.jobe.2021.102174
- Anwar A, Liu X, Zhang L. (2023). *Nano-cementitious composites modified with Graphene Oxide – a review*. Thin-Walled Struct, 183, 110326. doi:10.1016/j.tws.2022.110326
- Chuah S, Pan Z, Sanjayan JG, Wang CM, Duan WH. (2014). *Nano reinforced cement and concrete composites and new perspective from graphene oxide*. Constr Build Mater, 73, 113-124. doi:10.1016/j.conbuildmat.2014.09.040
- Anwar A, Mohammed BS, Wahab MA, Liew MS. (2020). *Enhanced properties of cementitious composite tailored with graphene oxide nanomaterial - A review*. Dev Built Environ, 1, 1-21. doi:10.1016/j.dibe.2019.100002
- Pettitt ME, Lead JR. (2013). *Minimum physicochemical characterisation requirements for nanomaterial regulation*. Environ Int, 52, 41-50.
- Muthu M, Ukrainczyk N, Koenders E. (2021). *Effect of graphene oxide dosage on the deterioration properties of cement pastes exposed to an intense nitric acid environment*. Constr Build Mater, 269, 121272. doi:10.1016/j.conbuildmat.2020.121272
- Li Z, Young RJ, Wang R, et al. (2013). *The role of functional groups on graphene oxide in epoxy nanocomposites*. Polymer (Guildf), 54(21), 5821– 5829. doi:10.1016/j.polymer.2013.08.026
- Standards Australia. (2010). *AS 3972-2010: General Purpose and Blended Cements*. Vol Third.
- Standards Australia. (2001). *AS 3582.2 - 2001: Supplementary Cementitious Materials for Use with Portland and Blended Cement Part 2 : Slag – Ground Granulated Iron Blast-Furnace*.
- Standards Australia. (1998). *AS 3582.1-1998: Supplementary Cementitious Materials for Use with Portland and Blended Cement Part 1 : Fly Ash*.
- AS 1478.1. (2000). *Chemical Admixtures for Concrete , Mortar and Grout Part 1 : Admixtures for Concrete*.
- AS/NZS 4058 (2007). *AS/NZS 4058:2007 - Precast Concrete Pipes (Pressure and Non-Pressure)*.
- BS EN 206 (2013). *BS EN 206:2013 - Concrete — Specification , Performance , Production and Conformity*.
- Matějková P, Matějka V, Sabovčík T, Gryžbon L, Vlček J. (2022). *Alkali Activation of Ground Granulated Blast Furnace Slag and Low Calcium Fly Ash Using “ One - Part ” Approach*. J Sustain Metall, 8, 511-521.
- Ren J, Zhang L, San Nicolas R. (2020). *Degradation process of alkali-activated slag/fly ash and Portland cement-based pastes exposed to phosphoric acid*. Constr Build Mater, 232, 117209. doi:10.1016/j.conbuildmat.2019.117209
- Koenig A, Dehn F. (2016). *Main considerations for the determination and evaluation of the acid resistance of*

- cementitious materials*. Mater Struct, 49, 1693-1703. doi:10.1617/s11527-015-0605-7
- BS EN 14630 (2006). *Products and Systems for the Protection and Repair of Concrete Structures — Test Methods — Determination of Carbonation Depth in Hardened Concrete by the Phenolphthalein Method*.
- Ren J, Zhang L, Walkley B, Black JR, San R. (2022). *Degradation resistance of different cementitious materials to phosphoric acid attack at early stage*. Cem Concr Res, 151, 106606. doi:10.1016/j.cemconres.2021.106606
- Gu L, Visintin P, Bennett T. (2020). *Sulphuric Acid Resistance of Cementitious Materials: Multiscale Approach to Assessing the Degradation*. J Mater Civ Eng, 32(7), 04020171. doi:10.1061/(asce)mt.1943-5533.0003261
- Aboulela A, Lavigne MP, Buvignier A, et al. (2021). *Laboratory test to evaluate the resistance of cementitious materials to biodeterioration in sewer network conditions*. Materials (Basel), 14(3), 1-24. doi:10.3390/ma14030686
- Lv S, Ma Y, Qiu C, Sun T, Liu J, Zhou Q. (2013). *Effect of graphene oxide nanosheets of microstructure and mechanical properties of cement composites*. Constr Build Mater, 49, 121-127. doi:10.1016/j.conbuildmat.2013.08.022
- Habibnejad Korayem A, Ghoddousi P, Shirzadi Javid AA, Oraie MA, Ashegh H. (2020). *Graphene oxide for surface treatment of concrete: A novel method to protect concrete*. Constr Build Mater, 243, 118229. doi:10.1016/j.conbuildmat.2020.118229